FORMATION AND DISTRIBUTION OF NUCLEAR PORE COMPLEXES IN INTERPHASE

GERD G. MAUL, JOSEPH W. PRICE, and MICHAEL W. LIEBERMAN

From the Department of Pathology and Fels Research Institute, Temple University School of Medicine, Philadelphia, Pennsylvania 19140

ABSTRACT

The possibility of nuclear pore formation in the interphase nucleus was investigated in control and phytohemagglutinin (PHA) stimulated lymphocytes by the freeze-etching technique. 48 hr after the addition of PHA, the newly formed blasts which had not as yet divided had at least twice the number of pores per nucleus as controls. This clearly demonstrates that in lymphocytes nuclear pore formation can take place during interphase.

It has generally been assumed that the distribution of nuclear pore complexes in somatic animal cells is random. However, we have utilized freeze etched rat kidney cells and a computer program to evaluate pore distribution. We find a minimum pore center-to-center spacing of approximately 1300 A and multiples thereof with high frequency. This is strong evidence for a nonrandom distribution of nuclear pores. The nonrandomness may be related to an underlying chromosomal organization in interphase.

Using three criteria for identifying prospective pore sites (membrane specialization, nonrandomness, and alteration of heterochromatin distribution), we have found forming pores in sectioned material from cultured human melanoma cells. While nuclear pore formation may take place in conjunction with reformation of the nuclear membrane, a mechanism also exists for their formation during interphase.

INTRODUCTION

A crucial aspect of cellular organization in eukaryotes is the regulation of nucleo-cytoplasmic information transfer. Despite its central role in cellular processes, almost nothing is known about the mode of nuclear entrance or exit of information-containing macromolecules or so-called small molecule messengers (e.g., biologically active peptides, steroids, cyclic adenosine monophosphate[AMP]). Because the nuclear pore is likely to be related to some or all of these processes, we have begun an investigation of the role of the nuclear pore in cellular processes (14, 15). While many of the structural details of the nuclear pore are known (for review see reference 9), few functional studies are available. Feldherr (6, 7), however, has demonstrated that colloidal gold of the approximate size of macromolecules can pass through the pore complex and that such movement is not a function of pore area. The movement of colloidal gold was dependent on the nuclear activity and seemingly regulated by electron-opaque material associated with the pore.

In this communication we demonstrate that nuclear pores can be formed during the interphase when cellular macromolecular metabolism is altered and that pores in interphase nuclei have a nonrandom distribution. Structural evidence for nuclear pore formation will also be presented.

MATERIALS AND METHODS

Freshly drawn blood was sedimented with 3% pig skin gelatin (4). The serum was the passed through a nylon column as described by Cooper et al. (3). This resulted in a preparation of lymphocytes, 99% free of other leucocytes. Two samples of 1.2×10^6 lymphocytes/ml were suspended in modified Eagle's medium with 15% fetal calf serum containing 10 units/ml of penicillin and streptomycin. Glutamine was added to a concentration of 2 mM. The control cells were frozen in liquid nitrogen-cooled Freon 22 after 1 hr of incubation in 20% glycerol in Eagle's medium at 0°C. A sample was incubated for 48 hr in the presence of 15 μl/ml of Difco phytohemagglutinin M (Difco Laboratories, Inc., Detroit, Mich.) to stimulate blast transformation. The cells were then processed as described for the control. Previous experiments in our laboratory showed no mitotic figures at this time. Radioautographic results indicate that 0.1–0.2% of the cells are labeled after incubation with tritiated thymidine (11). The specimens were freeze-etched according to Moor and Mühlenthaler (17) in a Balzer apparatus at 100°C. Etching time was 2 min. The exposed surface was then shadowed with platinum and carbon coated. A calibrated Siemens 101 electron microscope was used to photograph the exposed nuclear surface areas at a fixed magnification of 10,000. The negatives were enlarged to 30,000, the pores were counted, and the areas of the exposed nuclear envelopes were determined by planimetry.

For the determination of nuclear pore distribution, rat kidney cells (cortex) were used because they have a higher frequency of nuclear pores/μ^2 than lymphocytes but do not approach the densest possible packing. Small tissue pieces were incubated in ice-cold 20% glycerol in Tyrodes' solution for 1 hr and processed as above. A Hitachi HU 11 C electron microscope was used to photograph the exposed nuclear envelope surface areas at 20,000. After photographic enlargement to 200,000 the centers of the pores were marked. The relative position of the pore centers was determined on a data digitalizing table (Thompson d-mac Ltd., Glasgow, Scotland) and processed by a PDP-12 laboratory computer (Digital Equipment Corp., Manyard, Mass.). The computer was programmed to calculate and sort distances between each pore and all other pores within a radius of 1 μ. No interpore distance was expressed more than once in the histogram plot. In order to keep the histogram comparable, the number of distances for each interval (100 A) was expressed as per cent of the total number of distances calculated.

For the structural analysis of nuclear pore formation, human melanoma cells in vitro were fixed for 1 hr at room temperature in Falcon plastic tissue culture flasks (Falcon Plastics, Division of B-D Laboratories, Inc., Los Angeles, Calif.) in 3% glutaraldehyde (19) in 0.1 M phosphate buffer (pH 7.4) which contained 3 mM $CaCl_2$. This fixation was followed by 1 hr in 1% OsO_4 in the same buffer. The cells were prestained in 0.25% uranyl acetate (10) in water and dehydrated and flat-embedded according to Brinkley et al. (1) in Epon 812 (13). Serial sections were cut with a diamond knife on an LKB ultratome, mounted on collodium-coated single-hole grids, stained in uranyl acetate and lead citrate (20), and examined with a Siemens 101 electron microscope at 80 kv.

RESULTS

Evidence for nuclear pore formation during Interphase

The following results were obtained by comparing the nuclear pore frequencies of unstimulated lymphocytes with those of lymphocytes which were stimulated with phytohemagglutinin (PHA) for 48 hr, i.e. before they had undergone mitosis. In Fig. 1 the distribution of nuclear pores of an unstimulated lymphocyte can be seen. An increase in pore number is readily apparent if Fig. 1 is compared with Fig. 2 which shows part of a nuclear envelope of a stimulated lymphocyte. In unstimulated lymphocytes a mean of 3.48 ± 0.17 nuclear pores/μ^2 of nuclear envelope was counted; in the stimulated lymphocytes it was 6.04 ± 0.33. Nuclear pores were counted on a total of 17 nuclear fragments with an average size of 14.5 μ^2 from unstimulated lymphocytes, and on 34 nuclear fragments with an average size of 14.2 μ^2 from stimulated lymphocytes. The difference in nuclear pore frequencies is statistically significant ($p < 0.001$). The variability in pore frequencies between different nuclei is rather small in the unstimulated lymphocytes, whereas the pore frequencies of nuclei of the stimulated lymphocytes show a wide variability (Fig. 3).

Change in pore number per nuclear area in itself does not establish that pores are newly formed; therefore, the surface area of the nucleus was estimated and used to calculate the total number of nuclear pores per nucleus. 100 nuclei from each group were measured with an ocular micrometer with phase optics after incubation in 20% glycerol for 1 hr. Two measurements were made at right angles to each other and averaged. The measurement was made in multiples of 0.75 μ. The measurement of the nuclei has to be regarded as an estimate. If anything, the estimates understate the difference between the two populations. Because

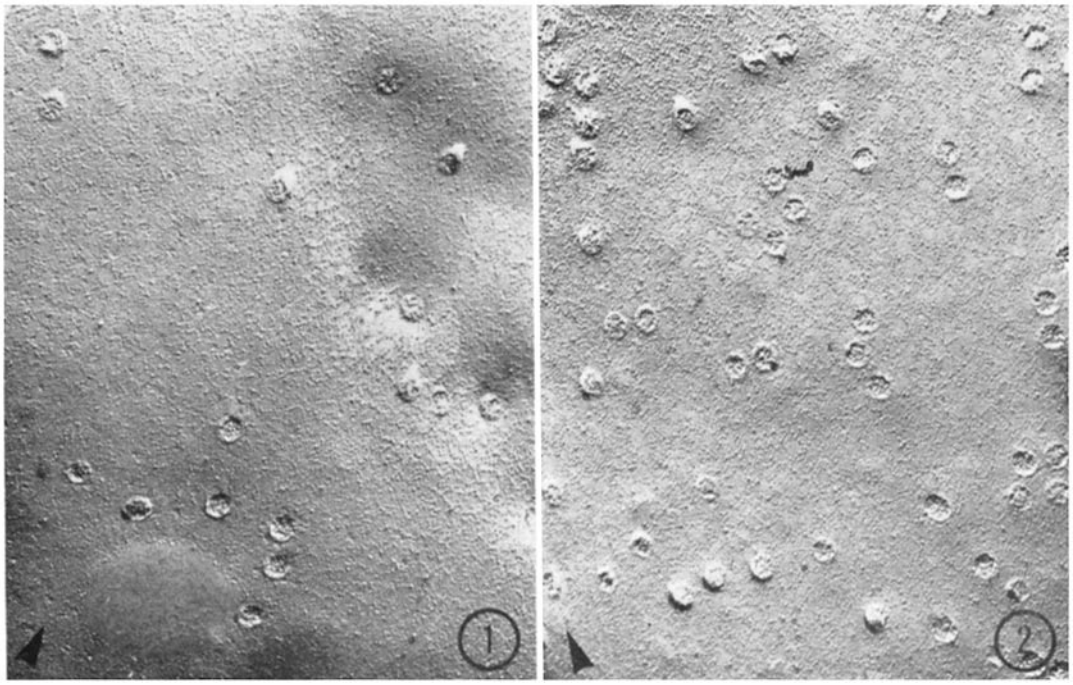

FIGURE 1 Nuclear membrane of an unstimulated lymphocyte. The inner nuclear membrane is seen from the cytoplasmic side. The magnification of this micrograph was used to count the nuclear pores. The direction of the shadowing is indicated by an arrow in the left lower corner of all micrographs of freeze-etched preparations. × 30,000.

FIGURE 2 Nuclear membrane of a lymphocyte stimulated for 48 hr with PHA. The inner nuclear membrane is seen from the cytoplasmic side. Many more nuclear pores per unit area are seen in this figure than in Fig. 1. × 30,000.

of the small distance between the nuclear membrane and the cell membrane, the exact size of the nucleus was often difficult to determine. In doubtful cases the large diameter was chosen. The surface of the nucleus was calculated as a sphere, using the average diameter. The nuclei of unstimulated lymphocytes had an estimated surface of 140 μ^2, whereas the surface of nuclei of stimulated lymphocytes was 180 μ^2. With the use of these estimates, the total number of nuclear pores can be calculated to be 490 and 1100, respectively. These figures suggest that in PHA-stimulated lymphocytes the number of nuclear pores is at least doubled before cell division takes place.

Evidence for the Nonrandom Distribution of Nuclear Pores

In Fig. 4 the exposed nuclear surface of a selected rat kidney nucleus (intracisternal aspect of the outer nuclear membrane) is shown. Pores with equal center-to-center spacing (±100 A) are connected by equal length lines. Circular areas which are devoid of membrane particles are seen on the nuclear membrane. These circular "bare areas" are larger than the nuclear pores, but can be connected with each other by equal lines of the same length. The pores 4–7 are arranged in a square, the sides of which have a length of 1300 A. This minimum distance is apparent throughout Fig. 4, not only between the centers of pores but also between the center of pores and the center of the circular bare areas. (7–15/–11; 20–26/–27; 22/–23/; 31–32/; numbers represent pores; numbers followed by a bar represent circular bare areas). A center-to-center spacing of approximately double the minimum distance appears with high frequency. (1–4; 3–6; 2–5; 6–13–17–24–29/–33/; 6–14–18/–25/; 21–19–26/; 20–22/–28/; 8/–12; 9–10; 7–16–11). The distance which is the equivalent

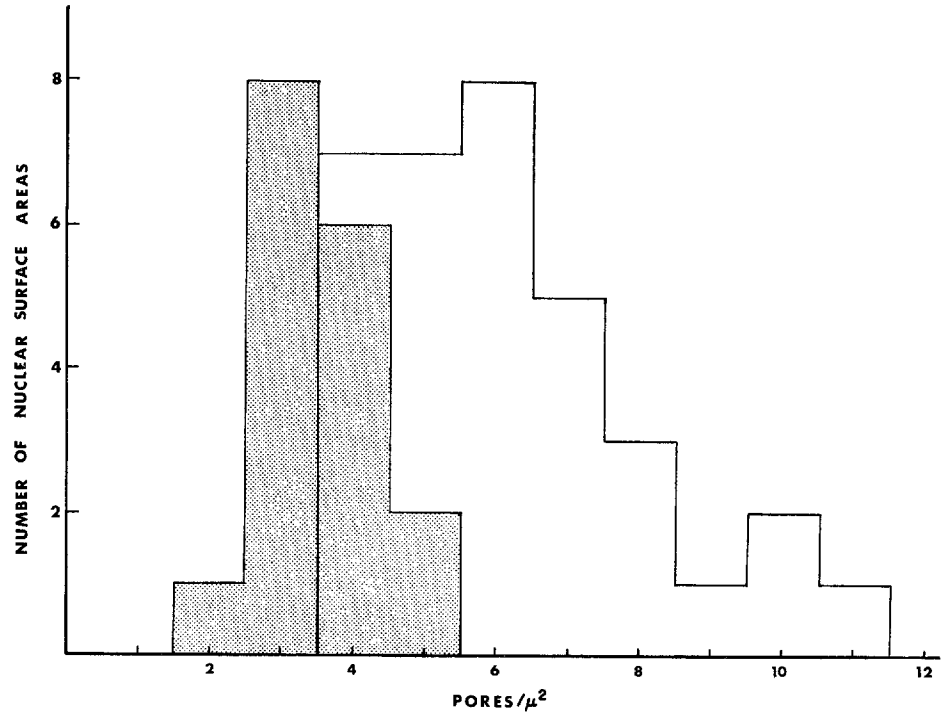

FIGURE 3 Histogram of pore frequencies/μ_2 as a function of nuclear surface areas counted. The shaded area represents the distribution of pore frequencies from nuclei of unstimulated lymphocytes (mean 3.48 ± 0.17*). The clear area represents the distribution of pore frequencies from stimulated lymphocytes (mean 6.04 ± 0.33*). The difference in nuclear pore frequency is statistically significant ($P < 0.001$). *, standard error of the mean.

of the diagonal through the square pattern (5–6) is also often found (1–2; 7–14; 15/–16–19–20; 24–25/). Multiples of the minimum distance can be seen between 1–5; 3–7; 19–27; 20–23; 30–33/; (3×) and 3–17–29; 17–18–27–32/; 31–33/; (4×). It is apparent that a high number of equidistances are present between pores in this figure. This would not be so if the pores as well as the circular bare areas were randomly distributed.

In order to substantiate the apparent nonrandom distribution of nuclear pores, larger nuclear surfaces were analyzed. The pore center-to-center spacing from each pore to all other pores was calculated and plotted. However, each pore-to-pore distance was registered only once.

In order to assess the significance of each maximum on the histogram, point-to-point distances on a random point plot were analyzed. Random numbers (8) were used for the x and y axis of each point. The average frequency of pores of the rat kidney nuclei was imitated (~13.5 pores/μ^2; mean of three exposed nuclear envelope pieces with a combined pore number of 558). Each random point which was closer than the minimum pore-to-pore distance to another point was randomly eliminated when the numbers were plotted on graph paper. A hexagonal pattern was constructed on the same type of graph paper, using the minimum pore-to-pore distance as the sides of the hexagon.

Fig. 5 shows three histograms: (A) random "pore" distribution, (B) hexagonal "pore" distribution, and (C) the distribution of pores as found on the exposed surface of a rat kidney nuclear envelope. Plotting the distances between the randomly generated points results in a histogram which rises sharply from 1300 A to ~1700 A and then rises steadily.

The histogram obtained from distances between hexagonally arranged points (Fig. 5B) shows strong maxima at distances related to the base line of a hexagon and multiples thereof as well as of different types of diagonals and their multiples. Fig. 6 gives an illustration of the hexagonal ar-

FIGURE 4 Intracisternal aspect of the outer nuclear envelope of a rat kidney nucleus. Only the reappearing minimum distances between the center of nuclear pores and twice that distance are indicated by white lines. There are a number of other equidistances of high frequency which are described in the text. Membrane specializations such as the circular membrane particle-free areas and an indentation are also included in order to demonstrate that they fit into the spatial order obvious for pores. × 100,000.

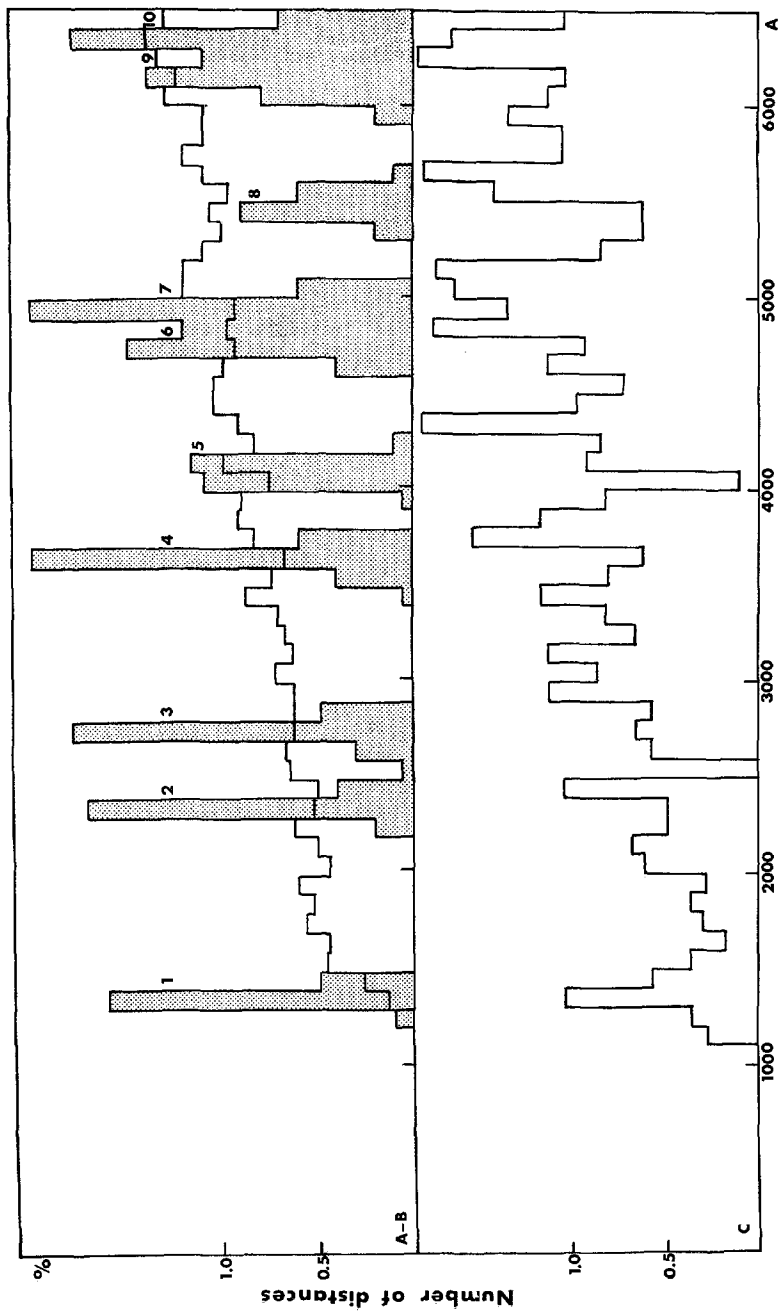

FIGURE 5 *Histogram of computer analyzed distances: A, distances between random points; B, hexagonally arranged points; C, between pore centers of a rat kidney nuclear envelope. The number of pore-to-pore distances is expressed as per cent of all distances calculated. Class interval is 100 A.*

	A	*B*	*C*
Number of pores	225	208	76
Number of distances calculated	3829	6797	1074
Pore frequency/μ^2	13.5	67	13.5

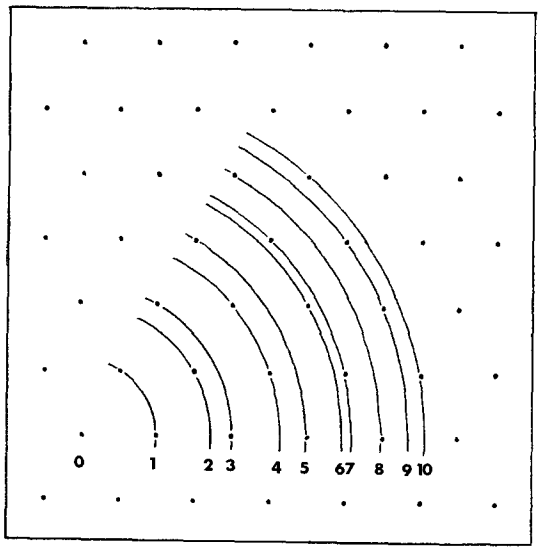

FIGURE 6 Illustration of distances represented in the histogram *5B* for hexagonally arranged points. The numbers correspond to the maxima. The frequency of 67 pores/μ^2 should be the maximum if the minimum pore-to-pore distance and pore diameter are constants.

rangement, the distances between points and their corresponding maxima. It also shows that at the densest possible packing, assuming a minimum pore center-to-center spacing of 1300 A, a maximum of 67 pores per μ^2 could possibly be found.

The width of the base of each maximum in the hexagonally arranged point-to-point distance plot (Fig. 5B) gives an indication of the error introduced by the width of the lines used to draw the hexagons and the accuracy with which the magnetic needle of the data digitalizing table can be placed. Errors of the same magnitude have to be expected by determining the pore centers.

If the nuclear pore-to-pore distances of a nucleus of a rat kidney cell are analyzed (Fig. 5C), one finds maxima at 1300 A, 2400 A, 3700 A, 4800 A–5200 A, and 6200 A, which could be regarded as multiples of ~1250 A. The data points represented as 1300 A are the sum of all distances between 1250 A and 1350 A. There is a minor maximum at 2000 A which must be regarded as significant in view of the distances equal to the diagonal of the squarely arranged pores in Fig. 4 (5–6). The extreme minima in the histogram also appear regularly. The distance from the first recorded distances (1100 A) to the first minimum (2500 A) is ~1500 A. The next one appears at 4000 A followed by one at 5400 A. If one follows the histogram up to 10,000 A, more maxima and minima are found but they are less convincing. Problems due to the curvature of the nuclear membrane, as shown in Fig. 7, become more apparent with larger distances. The analysis of this nuclear membrane (Fig. 7) which had approximately 200 pores also showed a strong initial maximum at 1300 A but with a much wider base and less distinct addi-

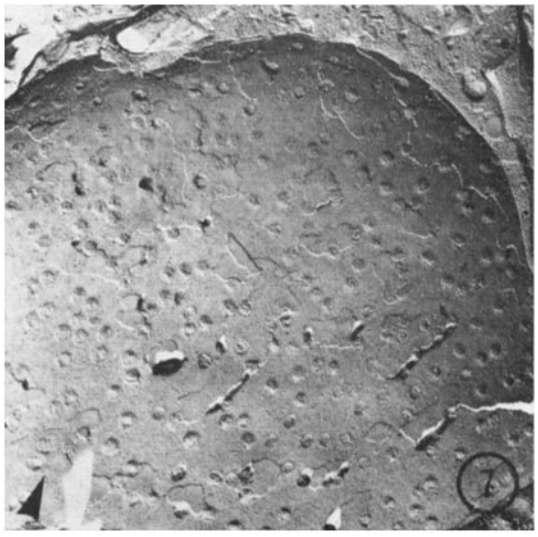

FIGURE 7 Rat kidney nucleus. With large nuclear envelope areas the distortion due to the curvature becomes apparent when distances between pores are analyzed. × 9000.

tional maxima. The extreme minima were not recognizable. If one compares the distribution of distances between hexagonally arranged points and the distribution of distances between pores, one finds a similar spacing between maxima. We tried to fit the data to other simple geometric patterns but none of these was satisfactory.

Structural Evidence of Nuclear Pore Formation

Because the circular bare areas on the nuclear membrane fit into the same nonrandom distribution as nuclear pores, as demonstrated in Fig. 4, we postulate that they may be forming or closing pores. If this is so, then one should also find an indication of forming pores in sectioned material.

Heterochromatin covers the inner nuclear membrane in dense 150–200 A wide strands except at the nuclear pores where heterochromatin-free areas exist which have approximately double the pore diameter (Fig. 8A, pore complexes 1–3). Such an area contains the nonmembranous part of the pore complex which consists partly of the projection of the eight transversing fibers which pass through the pore (Fig. 8A, pore complex 6, arrows). They are continuous and indistinguishable from chromatin (Fig. 8B, pore complex 3) (14, 15).

Because of the nonrandomness of nuclear pores, the double membrane of the nuclear envelope, and the special arrangement of heterochromatin around nuclear pores, three criteria were used to search for forming pores: (*a*) the prospective pore site should fit into the nonrandom pattern of the nuclear pores, i.e. it should have the minimum distance, or multiples thereof, to other pores, or another distance which can be repeatedly found. (*b*) it is assumed that the two membranes of the nuclear envelope have to fuse to form a pore, that is membrane specializations which suggest fusion should be found. (*c*) there should be an alteration in the heterochromatin arrangement that suggests dispersal at the prospective pore site.

Using these criteria, we sought membrane specializations on the nuclear membrane, the center of which had common distances from other pores and reduced heterochromatin or heterochromatin-free areas at the corresponding nucleoplasmic site as seen in a consecutive serial section. Fig. 8 is an example of such a finding. Pore complexes 4–5 and 9–10 are separated by the minimum distance. Between pore complexes 5 and 8 a polysome is situated which also has the minimum distance to both pores (the relationship of polysomes to nuclear pores will be described in a subsequent communication). An electron-opaque area is situated at the minimum distance from pore complex 13. This area has its heterochromatin-free equivalent at the same site in the consecutive serial section (Fig. 8B). One can recognize structures of the nonmembranous part of the pore complex. There is an electron-opaque membrane area (11) separated from pore complexes 8 and 14 by the same distance as 8 is separated from 10. It has its heterochromatin-free equivalent at the appropriate site in the consecutive section. It also shows a ringlike arrangement (the center is marked by a black dot) of chromatin fibers with chromatin attachments radiating to the heterochromatin (arrows). At the minimum distance from pore complex 14 (Fig. 8B) there is a heterochromatin ring (15). At the same site in Fig. 8A, a dense granule

FIGURE 8A–B Consecutive sections parallel to the nuclear membrane. Fig. 8A shows at the right half the nuclear envelope without heterochromatin, and at the left half the heterochromatin which is a thin layer of approximately 200–400 A thickness attached to the inner nuclear envelope (see cross section in Fig. 11). The absence of heterochromatin and the presence of the nonmembranous part of the nuclear pore complex can be seen at pores 1–3. The projection of the traversing fibers is indicated by arrows at pore 6. Prospective pore sites are marked 11, 12, 15. At the right of Fig. 8B, one can find the heterochromatin layer which corresponds to the nuclear membrane in Fig. 8A. At the left the chromatin arrangement of the layer immediately beneath the heterochromatin layer shows that one can still recognize the chromatin of the nonmembranous part of the nuclear pore complex (1–3, arrows). The prospective pore sites are recognizable as areas with less heterochromatin. × 100,000.

FIGURE 9A–B Consecutive sections parallel to the nuclear membrane. Electron-opaque circular area (5) on the nuclear membrane with a diameter approximating that of a nuclear pore is considered to be a prospective pore site. (See also cross section in Fig. 11). At the corresponding site in the consecutive section (9B), one finds a semicircle of cross-sectioned heterochromatin fibers (arrows). × 100,000.

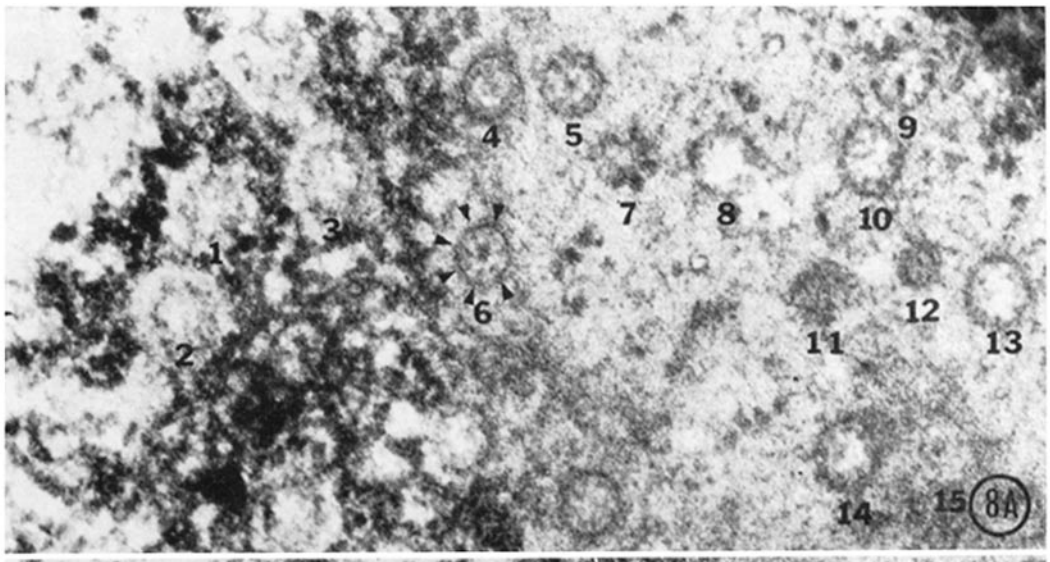
1
2
3
4
5
6
7
8
9
10
11
12
13
14
15
8A

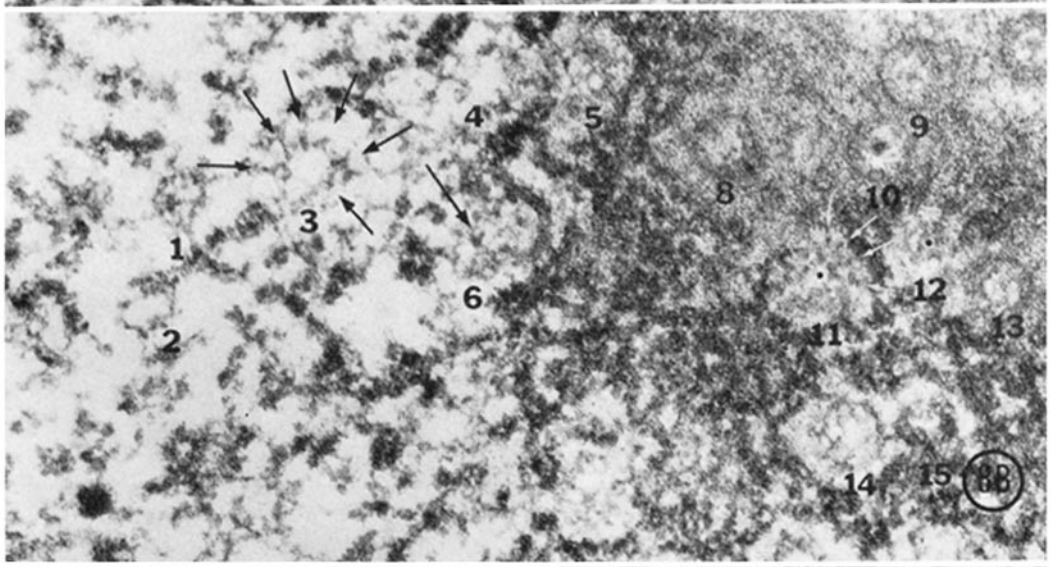
1
2
3
4
5
6
8
9
10
11
12
13
14
15
8B

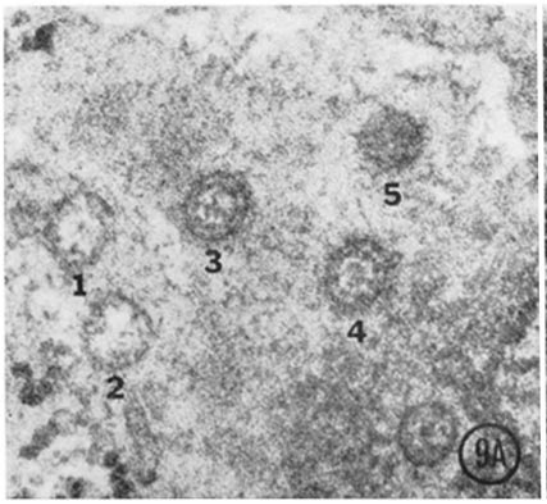
1
2
3
4
5
9A

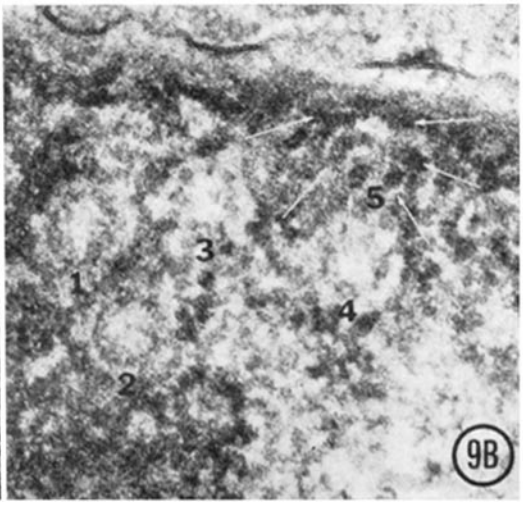
1
2
3
4
5
9B

as appears in pore complexes 5, 6, and 10 can be seen. In Fig. 9 the distance between pore complexes 1 and 3 is equal to the distance between pore complex 4 and the electron-opaque area 5. At the same area below the nuclear membrane, one can find a semicircle of more or less cross-sectioned heterochromatin fibers (arrow). The full circle cannot be seen due to the curvature of the nuclear membrane.

It is difficult to establish a morphological sequence of pore formation with the available material. But the differing images of nuclear-pore complexes (Fig. 10) suggests a possible sequence. Pore 4 in Fig. 10B is approximately equidistant from pores 1 and 2 and from the central granule at the prospective pore sites 3 and 5. In Fig. 10A there is a membrane specialization found at the corresponding site. At the prospective pore site 5, it appears as if the outer and inner nuclear membranes have already fused and partially disappeared. At the prospective pore site 3, only an electron-opaque area can be observed at the nuclear membrane. Both prospective pore sites, however, have a "central granule" and are not distinguishable at the heterochromatin level. If one assumes that these sites represent forming pores, the prospective pore site 3 should be an earlier stage than 5. The center of nuclear pore 7 is equidistant from pore 6 and from the centers of prospective pore sites 8 and 9 (Fig. 10B). There is a membrane specialization seen for the prospective pore site 9 but not for the prospective pore site 8. However, there is a very clear heterochromatin-free area and not much evidence for the nonmembranous part of the nuclear pore complex. These changes suggest that the membrane part of the nuclear pore complex has closed and separated before the heterochromatin has again been condensed and attached to this area.

The minimum distance or equidistances between nuclear pore complexes within a given micrograph were used for reference because the minimum distance in sectioned material (~1100 A) is smaller than the minimum distance found in freeze-etched preparations. This is thought to be due to shrinkage during dehydration.

As the outer and the inner nuclear membranes have to make contact and fuse during the assumed pore formation, cross sections should reveal such areas. If one also assumes that the induction takes place at specific chromatin sites on the inner nuclear membrane, then the inner nuclear membrane should protrude towards the outer nuclear membrane. The nuclear membrane usually appears rather wrinkled in sectioned material, and in such a state is unsuitable for analysis. The fixation, dehydration, and embedding procedures utilized for our material seem to minimize this effect. Fig. 11 shows a nuclear pore complex and, at the right, an indentation of the inner nuclear membrane (arrow). The base of this indentation corresponds to the width of the pore. Also, heterochromatin is absent at the area of the indentation in the same manner as at the nuclear pore complex. There are two strands of heterochromatin cross-sectioned between the nuclear pore complex and the prospec-

FIGURES 10A–B Face-on view of the nuclear envelope. Prospective pore sites are marked 3, 5, 8, 9. Their relationship to pores is described in the text. In Fig. 10B, prospective pore sites 3 and 5 can be seen to contain a central granule. Prospective pore site 8 is present only as an area without heterochromatin and does not have a corresponding membrane specialization. A membrane density, however, is present at 9 (Fig. 10A). × 100,000.

FIGURE 11 Cross section of a nuclear envelope. Note that the obliquely sectioned nuclear envelope is straight. There is a nuclear pore complex with electron-opaque material on the cytoplasmic side. An indentation of the inner nuclear envelope which has the same base width as the pore can be seen to the right (arrow). Heterochromatin is not present at this prospective pore site but it surrounds the indentation in the same way that it does the nuclear pore complex. × 150,000.

FIGURES 12 and 13 Inner nuclear membrane as seen from the nucleoplasm. In PHA-stimulated lymphocytes, one can find indentations of the inner nuclear membrane. They correspond to the indentation found in sectioned material (Fig. 11).

FIGURE 14 Outer nuclear membrane as seen from the nucleoplasm. No membrane indentations are found on the outer nuclear membrane. Circular bare areas are seen which might correspond to these indentations. Both circular bare areas have approximately the same distance from the closest pore. × 60,000.

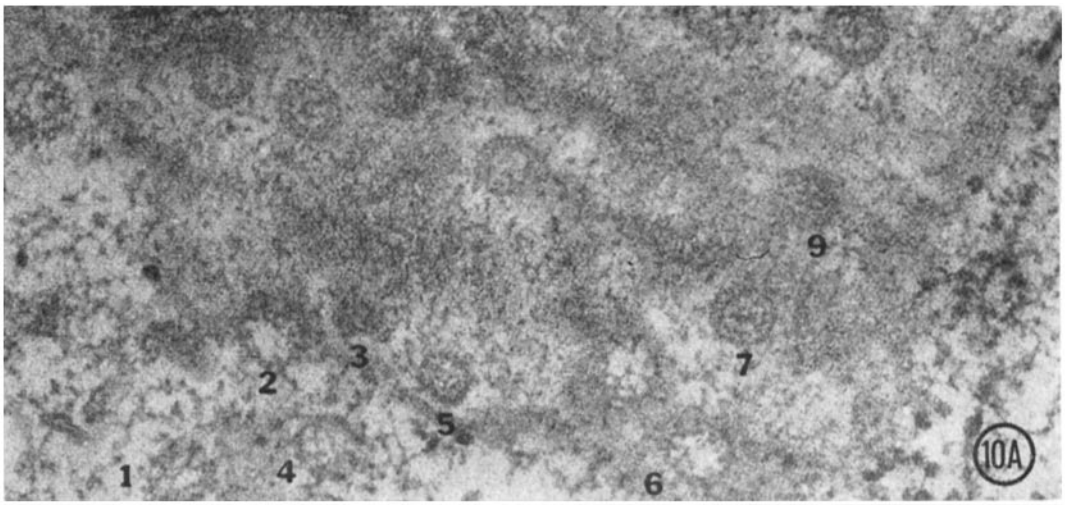
1
2
3
4
5
6
7
9
10A

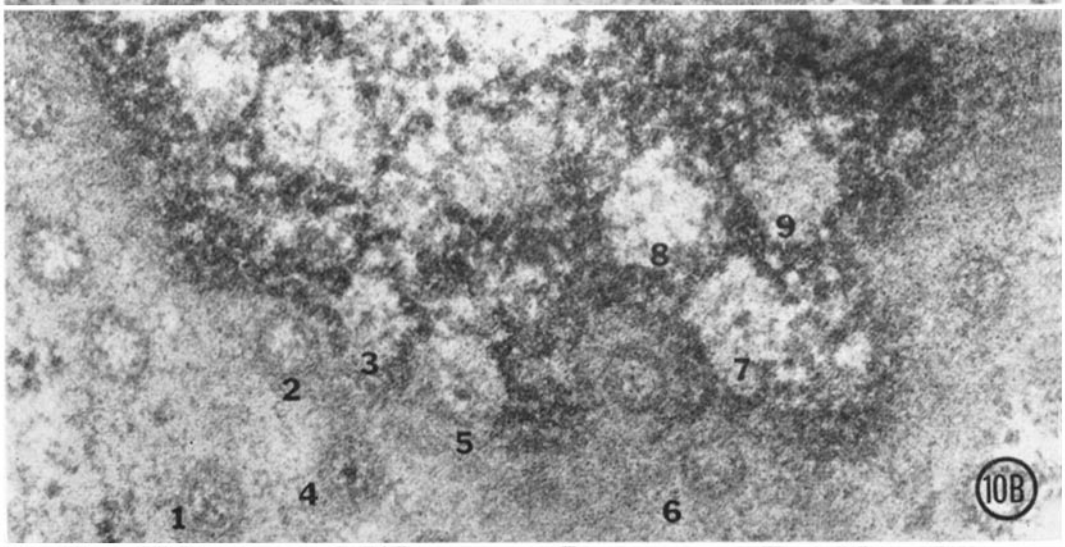
1
2
3
4
5
6
7
8
9
10B

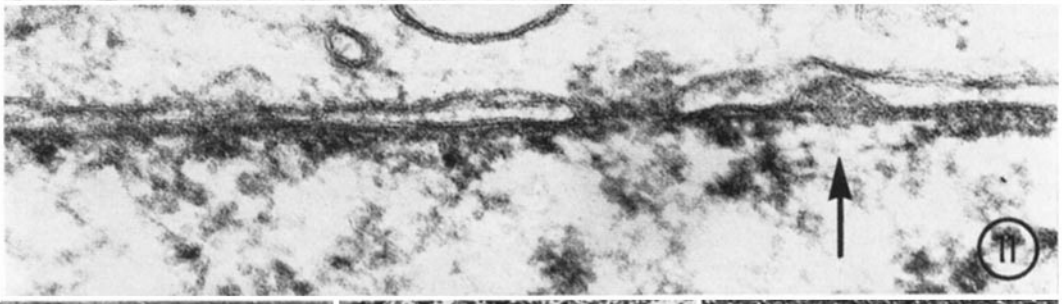
11

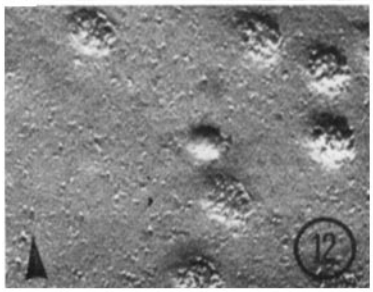
12

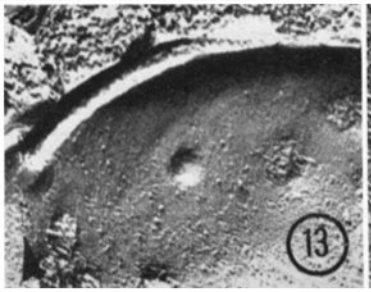
13

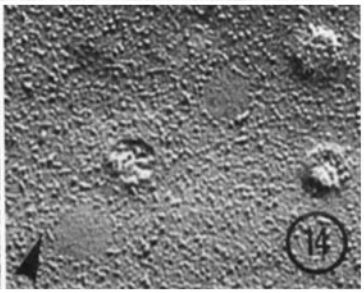
14

tive pore site. The nuclear membrane is obliquely sectioned.

If freeze-etched nuclear membranes of stimulated lymphocytes are searched for indentations, they can be found at the inner nuclear membrane as seen from the nucleoplasm (Figs. 12 and 13). No such indentations could be observed on the outer nuclear membrane, but small, circular, bare areas, slightly larger than the cross-fractioned nuclear pores, were found if the outer nuclear membrane was viewed from the nuclear side (Fig. 14). They are assumed to be the same structures as the circular bare areas in the outer membrane of the rat kidney nuclei (Fig. 4). Their relationship to the indentations of the inner nuclear membrane is not clear.

DISCUSSION

It is generally accepted that nuclear pores are formed during the reformation of the nuclear envelope after mitosis and seem to be an obvious pathway for nucleo-cytoplasmic exchange of macromolecules. That the nuclear pores are used in the passage of particles of the general size of macromolecules was demonstrated by Feldherr (6). Most of the investigations on nuclear pore complexes were therefore concerned with the structure and frequency of nuclear pores. Feldherr (7) found that colloidal gold was incorporated into the nuclei of amoeba at a significantly higher rate than into oocyte nuclei. He assumed that neither the pore area nor the pore frequency are the determining factors for differing permeability but that the nonmembranous part of the nuclear pore complex is somehow involved.

The possibility that the number of pores per nucleus is variable within one cell type during interphase has been investigated by us as a possible control mechanism for information exchange.

Our initial investigations were carried out on lymphocytes because of the dramatic change from a relatively resting population to a metabolically active one during PHA-induced blast transformation. The striking increase in RNA and protein synthesis during blast transformation (12) is highly suggestive that such transfer actually takes place.

The average number of pores per nucleus in stimulated lymphocytes is twice the number of the control. This result needs qualification for two reasons. First, not all lymphocytes respond to PHA stimulation. Therefore, the average pore frequency is an underestimate of that present in stimulated cells. This interpretation is supported by the rather asymmetrical shape of the distribution curve (Fig. 3) and the wide variability of pore frequencies between different nuclei of stimulated lymphocytes. Furthermore, one could also imagine that the variability of pore frequencies reflects different degrees of stimulation.

The total number of pores per nucleus has to be regarded as an estimate because of the difficulty of accurately measuring the diameter of the nuclei. The high nucleocytoplasmic ratio leaves only a very thin cytoplasmic rim (often less than 0.5 μ) around the nucleus, which makes the distinction between nuclear membrane and cell membrane difficult. The average nuclear diameter of the PHA-stimulated lymphocytes is only 1 μ larger than the diameter of unstimulated lymphocytes. Since the unstimulated lymphocytes within the PHA-treated group are included in the average diameter, one might assume that the transformed cells have a larger average nuclear diameter than our value indicates. Because of the foregoing, we suggest that the ratio between the total pores per nucleus of unstimulated and stimulated lymphocytes is larger than 1:2. Since the lymphocytes have not undergone mitosis (12; Maul and Liebermann, unpublished results), nuclear pore formation must have taken place during interphase.

Nuclear pores were considered to be randomly scattered over the nuclear surface (5). Exceptions to the apparent random distribution of nuclear pores were reported for *Drosophila* and *Chironomus* salivary gland and *Xenopus* and *Triturus* oocytes (21), for nuclei of amoeba (16, 18), and for nuclei of *Tetrahymena* (22). These exceptions are due to hexagonal pore distributions (densest possible packing). Randomness of pore distribution at pore frequencies which are well below the maximum (as determined by hexagonal packing with a given minimum pore-to-pore distance) has not been demonstrated, but nonrandomness can also exist where a basic simple regular pattern is not obvious. This fact is clearly demonstrated by our data from the rat kidney nuclei. Here the comparison of point-to-point distances of a random point plot and of pore-center–to–pore-center distances in a nuclear envelope makes it obvious that nuclear pores are nonrandomly distributed. However, we have not as yet been able to determine their distribution pattern.

The minimum distance between two pore centers may be due to physical restraints. This, how-

ever, does not exclude the possibility of a gradually enlarging distance between pores. A demonstration of this is seen in the histogram of randomly arranged points after removal of all points closer than the minimum pore-to-pore distance (Fig. 5B). Therefore, the first maximum establishes the nonrandom distribution of nuclear pores. This is substantiated by the presence of maxima at multiples of the minimum distance. Despite the similarity of the histograms of the pore-to-pore distances and the point-to-point distances within a hexagonal pattern, we do not claim that nuclear pores are arranged in a basic regular pattern, since, if we tried to construct a hexagonal pattern with the pores present, we did not succeed for more than five pores covering an area of ~25 prospective pore sites.

The basic organizational pattern of nuclear pores may be related to the distribution of chromosomal material in the interphase nucleus. This suggestion is based on our observation of nonrandomness of nuclear pore distribution. Because chromatin fibers have been found by us (14, 15) and by Comings and Okada (2) to be attached in a highly regular manner to the nuclear pore rim, we suggest that nuclear pore distribution is somehow related to the organization of chromosomes during interphase. However, a possibility which we cannot as yet rule out is pore formation on some other basis and secondary attachment of chromatin.

Utilizing the nonrandomness of pore distribution, we have been able to localize prospective pore sites. In the process of pore formation the two opposing membranes have to fuse and dissolve in an orderly fashion. Thus, for a short time the two unit membranes are very close and therefore will appear as an electron-opaque circumscribed area when otherwise only one membrane is present in the section. Such areas were found and can be shown to have heterochromatin-free areas on their nucleoplasmic side. Therefore, we suggest a number of criteria for forming nuclear pore complexes: (*a*) they should fit into the nonrandomness established for nuclear pore complexes; (*b*) there should be (transitory) membrane specialization; and (*c*) heterochromatin should be absent or arranged differently than it is on the rest of the nuclear membrane and possibly reminiscent of that seen in pore complexes. At the present time we cannot distinguish between forming and closing pores.

The fact that nuclear pores may be formed during interphase and the possibility that they can disappear indicate a regulatory function. This regulatory function may simply be the control of the total pore area available for nucleocytoplasmic exchange. On the other hand, the finding that eight chromatin (2, 14, 15) fibers attach to the pore rim indicates that, in addition to a selective filter function for macromolecules, other regulatory mechanisms may reside at the nuclear pore complex.

We would like to thank Dr. Daniel Branton, Department of Botany, University of California, Berkeley, California, for the use of his laboratory and equipment to obtain the replicas used in this investigation. Miss Susan Whittock, Miss Patricia Jones, Miss Patricia Stranen, and Mr. Peter Delaney provided expert technical assistance. We are grateful to Dr. Emmanuel Farber in whose laboratory part of this work was done.

This investigation was supported by National Institutes of Health Grants CA-11654, CA-12680, CA-11511, CA-12218, and HE-08886, and American Cancer Society Grants JN88 and E-129M.

Received for publication 16 March 1971, and in revised form 23 April 1971.

REFERENCES

1. BRINKLEY, B. R., P. MURPHY, and L. C. RICHARDSON. 1967. Procedure for embedding *in situ* selected cell cultures *in vitro*. *J. Cell Biol.* **35**:279.
2. COMINGS, D. E., and T. A. OKADA. 1970. Association of chromatin fibers with the annuli of nuclear membranes. *Exp. Cell Res.* **62**:293.
3. COOPER, H. L., and A. D. RUBIN. 1965. RNA metabolism in lymphocytes stimulated by phytohemagglutinin: Initial responses to phytohemagglutinin. *Blood.* **25**:1014.
4. COULSON, A. S., and D. G. CHAMBERS. 1964. Separation of viable lymphocytes from human blood. *Lancet.* **1**:468.
5. DUPRAW, E. J. 1970. *In* DNA and Chromosomes Holt, Rinehart and Winston Inc., New York.
6. FELDHERR, C. M. 1964. Binding within the nuclear annuli and its possible effect on nucleocytoplasmic exchanges. *J. Cell Biol.* **20:** 188.
7. FELDHERR, C. M. 1969. A comparative study of nucleocytoplasmic interactions. *J. Cell Biol.* **42**:841.
8. FISHER, R. A., and F. YATES. 1957. Statistical tables for biological agricultural and medical research. Hafner Publishing Company Inc., New York. 5th edition. 126.
9. FRANKE, W. W. 1970. On the universality of the

nuclear pore complex structure. *Z. Zellforsch. Mikrosk. Anat.* **105**:405.

10. KELLENBERGER, E., A. RYTER, and J. SÉCHAUD. 1959. EM Studies of DNA-containing plasms. *J. Biophys. Biochem. Cytol.* **4**:671.
11. LIEBERMAN, M. W., R. N. BANEY, R. E. LEE, S. SELL, and E. FARBER. 1971. Studies on DNA repair in carcinogenesis: stimulation of thymidine incorporation by human peripheral blood lymphocytes treated with alkylating agents and proximate carcinogens. *Cancer Res.* **31**:1297.
12. LING, N. R. 1968. *Lymphocyte Stimulation.* North Holland Publishing Company, Amsterdam.
13. LUFT, J. H. 1961. Improvements in epoxy resin embedding methods. *J. Biophys. Biochem. Cytol.* **9**:409.
14. MAUL, G. G. On the octagonality of the nuclear pore complex. *J. Cell Biol.* **51**:558.
15. MAUL, G. G. 1970. The relationship of nuclear pores to chromatin. *J. Cell Biol.* **47** (2, Pt. 2): 132 a. (Abstr.)
16. MERRIAM, R. W. 1962. Some dynamic aspects of the nuclear envelope. *J. Cell Biol.* **12**:79.
17. MOOR, H., and K. MÜHLETHALER. 1963. Fine structure in frozen-etched yeast cells. *J. Cell Biol.* **17**:609.
18. PAPPAS, G. D. 1956. The fine structure of the nuclear envelope of *Amoeba proteus*. *J. Biophys. Biochem. Cytol.* **2** (Suppl.): 431.
19. SABATINI, D. D., K. BENSCH, and R. J. BARRNETT. 1963. Cytochemistry and electron microscopy. The preservation of cellular ultrastructure and enzymatic activity by aldehyde fixation. *J. Cell Biol.* **17**:19.
20. REYNOLDS, E. S. 1963. The use of lead citrate at high pH as an electron-opaque stain in electron microscopy. *J. Cell Biol.* **17**:208.
21. WIENER, J., D. SPIRO, and W. R. LOEWENSTEIN. 1965. Ultrastructure and permeability of nuclear membranes. *Cellule.* **66**:97.
22. WUNDERLICH, F., and W. W. FRANKE. Structure of macronuclear envelopes of *Tetrahymena pyriformis* in the stationary phase of growth. *J. Cell Biol.* **38**:458.